ROYAL SOCIETY
OF CHEMISTRY

RSC Advances

Interfacial tension of oil/water emulsions with mixed non-ionic surfactants: comparison between experiments and molecular simulations

P. Posocco, A. Perazzo, V. Preziosi, E. Laurini, S. Pricl and S. Guido

Experimental Methods

A homemade pendant drop apparatus was developed to characterise droplet interfacial tension (Figure 1). The latter is obtained by the axial symmetric droplet shape analysis (ADSA)[1] of a drop that is pending from a stainless steel capillary tube (external diameter: 1.5875 mm, internal diameter 1 mm). The drop is made of the less dense fluid and is immersed into the denser one. The phase where the drop is immersed is contained in a glass chamber (50 mm x 50 mm). Image analysis was performed also for the lighter phase immersed in the denser one but, in this case, the hook-shaped stainless steel needle was reverted, thus showing a drop "emerging or rising" from the capillary tip. We detected the drop shape by a digital camera Canon® EOS 60D having a resolution of 5184x3456 pixel equipped with a macro objective EF-S 60 mm. The dispersed phase was fed through the capillary tube by a syringe pump (Harvard Apparatus, PUMP 11 Plus Dual) and once the maximum drop volume was obtained, flow was stopped and the droplet profile analysed. We kept the pendant drop aligned between the light source and the camera. Temperature room was maintained at 25°C. A software based on axi-symmetric droplet shape profiles has been developed in Matlab®.
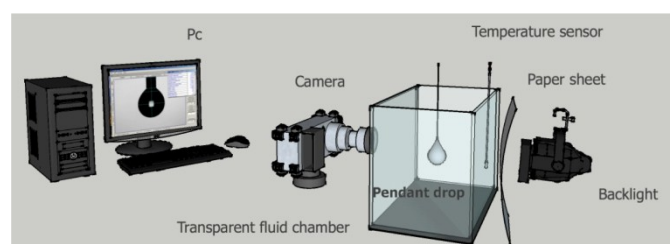

Figure 1. Experimental pendant drop apparatus.

Computational Methods

Dissipative Particle Dynamics (DPD)

The DPD model consists of N particles (or beads, i.e. clusters or groups of atoms or molecules) moving in a continuum domain of volume V. The time evolution of the particles of mass m_i is governed by Newton's equations of motion which have been set out in detail by Moeendarbary et al.[2] and by Groot and Warren[3] (Equation 1)

$$\frac{dr_i}{dt} = v_i \qquad \frac{dv_i}{dt}m_i = F_i$$

where r_i, v_i, and F_i are the position, velocity, and total force vectors, respectively, acting on particle i. The total force exerted on a bead i contains three components, each of which is pairwise additive and lies along the lines connecting the centers of particles i and j: a conservative (F_{ij}^C), a dissipative (F_{ij}^D), and a random (F_{ij}^R) force. The latter two act like a thermostat conserving the total momentum and introducing Brownian motion into the system. The DPD technique is designed to obey Navier-Stokes equations of hydrodynamics and to rigorously sample the canonical ensemble. Accordingly, the effective force F_{ij} acting on a particle i is given by (Equation 2):[3]

$$F_{ij} = F_{ij}^C + F_{ij}^D + F_{ij}^R$$

$$F^C(r_{ij}) = \begin{cases} a_{ij}(1 - r_{ij}/r_c)r_{ij} & r_{ij} \leq r_c \\ 0 & r_{ij} \geq r_c \end{cases}$$

$$F_{ij}^D(r_{ij}) = -\gamma\omega_D(r_{ij})(e_{ij}v_{ij})e_{ij}$$

$$F_{ij}^R(r_{ij}) = \sigma\omega_R(r_{ij})e_{ij}\xi_{ij}$$

where $r_{ij} = |r_i - r_j|$, $e_{ij} = r_{ij}/r_{ij}$ and $v_{ij} = (v_i - v_j)$.

The ξ_{ij} term is a Gaussian white noise function with symmetry properties (i.e. $\xi_{ij} = \xi_{ji}$). a_{ij} is the interaction parameter between particle i and j, and gives the strength for the repulsion between these two particles. ω_D and ω_R are the dissipative and random dependent weight functions that ensure that F^R and F^D vanish when r_{ij} becomes greater than r_c, a cut-off distance for forces. In analogy with the fluctuation-dissipation theorem, Español and Warren[4] obtained the detailed balanced condition for the DPD as (Equation 2):

$$\omega_D(r) = [\omega_R(r)]^2 \qquad \sigma^2 = 2\gamma k_B T/m$$

where γ is the friction coefficient, σ is the noise amplitude, k_B is the Boltzmann constant, and T the equilibrium temperature. The conservative force weight function is equal to $w_c(r_{ij}) = a_{ij}(1-r_{ij}/r_c)$ and zero otherwise. The dissipative and random weight functions take the general form (Equation 3)

$$\omega_D(r_{ij}) = [\omega_R(r_{ij})]^2 = \begin{cases} (1 - r_{ij}/r_c)^2 & r_{ij} \le r_c \\ 0 & r_{ij} \ge r_c \end{cases}$$

Finally, when modeling chains, another force is active in the system, i.e. a harmonic spring connecting two adjacent particles i and j (Equation 4):

$$F_{ij}^{bond} = K(r_{ij} - r_0)$$

where K is a spring constant and r_0 is the equilibrium distance between the particles.

Chain stiffness is modelled by a three body potential U^{angle} acting between adjacent bead triples ijz in a row using an angle bending potential in cosine form (Equation 5)

$$U_{ijz}^{angle} = \frac{1}{2}K_\theta[1 - cos(\theta_{ijz} - \theta_0)]$$

where K_ϑ is a spring constant and ϑ_0 is the equilibrium angle.

Computational Models

Tween 80 and Span 20 are commercial nonionic surfactants, whose final composition is a mixture of a number of chemical species. Thus, for instance polyoxyethylene (20) sorbitan – the major component of Tween 80 - can vary in number and type of hydrophobic tails, and/or number and distribution of ethoxylate units among the head groups. Basing on recent experimental evidence,[5] we assumed the "typical" structure for Tween 80 and Span 20 reported in Figure 2.
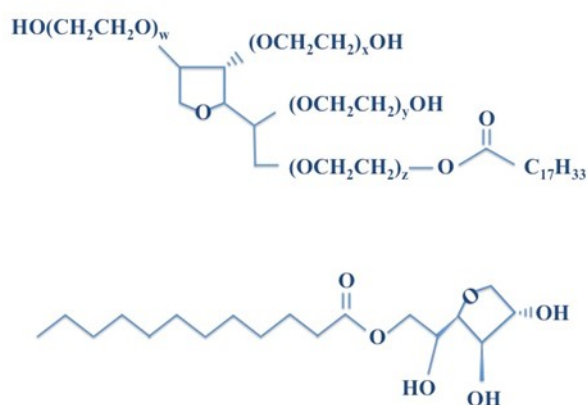

Figure 2. Typical structure of Tween 80 (top) and Span 20 (bottom). The ethoxylate head groups contain x, y, z, w number of ethylene oxide monomers here taken equal to 5.

The coarse-grained models for Tween 80 and Span 20 were obtained comparing the appropriate molecular dynamics (MD)/dissipative particle dynamics (DPD) pair-pair correlation

functions according to a procedure previously proposed and validated by our group.[6, 7] Briefly, a 1 μs MD simulation at 300 K was performed on one surfactant molecule in vacuum. The time step was 0.5 fs and the atomic interactions were described with the COMPASS force field[8]. Then, using the MD trajectory we computed the pair correlation function P between predefined atom groups (Equation 6)

$$P = \sum_i \sum_j \theta_{Ii}\theta_{Jj}\langle \delta(r_I - R_i)\delta(r_J - R_j)\rangle$$

where i and j are two atoms in the molecular fragments I and J, and <…> indicates a thermal average. ϑ_{ij} is a step function defined as (Equation 7)

$$\theta_{ij} = \begin{cases} 1 \; if \; i \; is \; of \; type \; I \\ 0 \; if \; i \; is \; not \; of \; type \; I \end{cases}$$

At the same time, we performed DPD simulations on the same, single molecule in vacuum. We employed a time step of 0.04τ. Every simulation was 5×10^5 step long, and every 100 steps the coordinates of the beads were stored, and then used to calculate the DPD pair correlation function according to Equation (6). By comparison of the MD/DPD pair correlation functions we determined if the assumed coarse-grain model was optimal. If not, we varied the bead number and architecture until the two distributions matched. Accordingly, we obtained the mesoscale model for Tween 80 and Span 20 shown in Figure 3, where bead types TT and TS represent the hydrophobic tail for Tween 80 and Span 20, respectively. The polar moiety is made of beads EO (polyoxyethylene units) and EOC (tetrahydrofuran group) for Tween 80, and H1 and H2 for Span 20, accounting for the different chemical components.
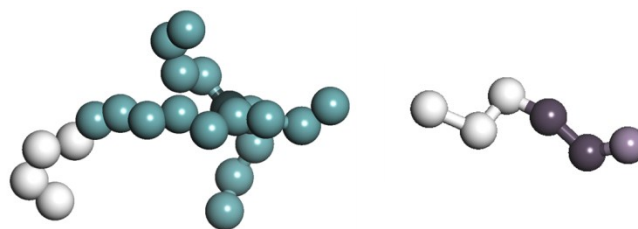

Figure 3. Mesoscopic models for Tween 80 (left) and Span 20 (right). Color legend: bead TT and TS, white; bead EO, light blue; bead EOC, dark blue; bead H2, dark purple; bead H1, purple.

Applying the same protocol described above we derived the DPD construct for the oil molecule, assuming dodecane as a prototype. Thus, a three-particle chain of bead type O was predicted. Finally, water molecules were represented by a single bead W.

According to the theory, the intra- and intermolecular interactions between DPD particles are expressed by the conservative parameter defined by Equation (2), which inherits the chemical information of the system. In this work, we employed a consolidated procedure that correlates the interaction energies estimated from atomistic MD simulations

to the mesoscale a_{ij} parameter values, rescaled onto the corresponding mesoscale segments.[6] To this purpose, adapting the original procedure to the present case, the atomistic interaction energies between the components were estimated from MD simulations of the corresponding mixture at 300 K. Briefly, after system energy minimisation, the mixtures were subjected to 2 ns equilibration in the isobaric-isothermal ensemble (NPT MD) at 300 K and 1 bar. Temperature and pressure control was maintained by the Berendsen thermostat and barostat.[9] Then, 4 ns production runs were carried out at constant volume and temperature (NVT MD). The time step was 1 fs in all simulations. The particle mesh Ewald[10] method was adopted in treating long-range electrostatic interactions, while a cutoff radius of 9.5 Å was assumed for all interactions. 100 snapshots were saved during the last 500 ps of the NVT MD production period described above for data analysis. The SPC/E model[11] was selected to represent water molecules. All MD simulations were performed with COMPASS force field.

The underlying procedure used to calculate the interaction energies and, hence, the binding energy values E_{bind} between all system components, is also well established.[12] Briefly, the binding energy of a system composed, for instance, of two components, A and B, is calculated from the following equation (Equation 8)

$$E_{bind}^{A-B} = E_A + E_B - E_{A-B}$$

where the first two terms represent the energy of A and B, consisting of both valence and non-bonded energy terms, and the last term is the interaction energy between the two components, made up of non-bonded terms only. By definition, the binding energy E_{bind} is the negative of interaction energy.

Once obtained, the atomistic interaction energies were rescaled onto the corresponding mesoscale segments averaging on the reciprocal number of contacts.[13] Here, the self-repulsive interaction parameters for water and oil were set equal to a_{W-W} = 25 k_BT/r_c and a_{O-O} = 75 k_BT/r_c, respectively, based on the direct relationship with their isothermal compressibility at room temperature.[14] Once these parameters were assigned, the entire bead–bead interaction parameter set for the DPD simulations was easily derived starting from the atomistic interaction energies values. Thus, water-oil interaction was a_{W-O}=96 k_BT/r_c. Self-repulsive interactions were represented by a_{EO-EO}=29, $a_{EOC-EOC}$=33, a_{H1-H1}=32, a_{H2-H2}=29, a_{TT-TT}=35, a_{TS-TS}=33 in k_BT/r_c units. Interaction with water was described by the following set: a_{EO-W}=26, a_{EOC-W}=32, a_{H1-W}=31, a_{H2-W}=28, a_{TT-W}=79, and a_{TS-W}=82, whilst interaction with oil by a_{EO-O}=48, a_{EOC-O}=58, a_{H1-O}=56, a_{H2-O}=52, a_{TT-O}=26, and a_{TS-O}=23. Finally, the mixed conservative parameters were set to a_{EO-EOC}=24, a_{H1-EO}=28, a_{H1-EOC}=31, a_{H2-EO}=26, a_{H2-EOC}=34, a_{H2-H1}=36, a_{EO-TT}=53, a_{EOC-TT}=57, a_{H1-TT}=60, a_{H2-TT}=55, a_{EO-TS}=50, a_{EOC-TS}=55, a_{H1-TS}=58, a_{H2-TS}=57, a_{TT-W}=79, and a_{TS-TT}=29.

We performed all calculations in a simulation box of area ~ 15 nm x 15 nm, with periodic boundary conditions. The enclosed systems were composed of approximately 1:4 oil:water weight ratio. The cut-off radius r_c, particle mass m, and k_BT were taken as scale units. A time step of $0.02\,\tau$ was chosen to safe guard numerical consistency for interfacial tension. Each DPD simulation consisted of an equilibration period of 100000 steps, followed 7-10 × 10^5 DPD step production runs, depending on the system involved and temperature standard deviation (k_BT) equilibration.

References

1. M. Hoorfar and A. W. Neumann, *Adv. Colloid Interface Sci.*, 2006, **121**, 25-49.
2. E. Moeendarbary, T. Y. Ng and M. Zangeneh, *Int. J. Appl. Mech.*, 2009, **1**, 737-763.
3. R. D. Groot and P. B. Warren, *J. Chem. Phys.*, 1997, **107**, 4423.
4. P. Espanol and P. Warren, *Europhys. Lett.*, 1995, **30**, 191.
5. R. Zhang, Y. Wang, Y. Ji, B.-j. Shi, Z.-p. Zhang, H.-y. Zhang, M. Yang and Y.-m. Wang, *J. Chromatogr.*, 2013, **1272**, 73-80.
6. G. Scocchi, P. Posocco, J. W. Handgraaf, J. G. E. M. Fraaije, M. Fermeglia and S. Pricl, *Chem. Eur. J.*, 2009, **15**, 7586-7592.
7. P. Posocco, M. Fermeglia and S. Pricl, *J. Mater. Chem.*, 2010, **20**, 7742-7753.
8. H. Sun, *J. Phys. Chem. B*, 1998, **102**, 7338-7364.
9. H. J. C. Berendsen, J. P. M. Postma, W. F. van Gunsteren, A. DiNola and J. R. Haak, *J. Chem. Phys.*, 1984, **81**, 3684-3690.
10. A. Toukmaji, C. Sagui, J. Board and T. Darden, *J. Chem. Phys.*, 2000, **113**, 10913-10927.
11. H. J. C. Berendsen, J. R. Grigera and T. P. Straatsma, *J. Phys. Chem.*, 1987, **91**, 6269-6271.
12. R. Toth, A. Coslanich, M. Ferrone, M. Fermeglia, S. Pricl, S. Miertus and E. Chiellini, *Polymer*, 2004, **45**, 8075-8083.
13. G. Scocchi, P. Posocco, M. Fermeglia and S. Pricl, *J. Phys. Chem. B*, 2007, **111**, 2143-2151.
14. H. Goel, P. R. Chandran, K. Mitra, S. Majumdar and P. Ray, *Chem. Phys. Lett.*, 2014, **600**, 62-67.